

KERNEL PCA-BASED RESOLUTION ENHANCEMENT APPROACH OF STILL IMAGES USING DIFFERENT LEVELS OF PYRAMID STRUCTURE

Takahiro Ogawa and Miki Haseyama

Graduate School of Information Science and Technology, Hokkaido University
Kita 14, Nishi 9, Kita-ku, Sapporo, Hokkaido, 060-0814, Japan
E-mail: ogawa@lmd.ist.hokudai.ac.jp, miki@ist.hokudai.ac.jp

ABSTRACT

This paper presents a kernel PCA-based adaptive resolution enhancement method of still images. The proposed method introduces two novel approaches into the kernel PCA-based reconstruction of high-frequency components missed from a high-resolution (HR) image. First, since local images between two different resolution levels of a pyramid structure are similar to each other, nonlinear eigenspaces of local images in the target low-resolution (LR) image are utilized as those of local images in the HR image. Further, in the kernel PCA-based reconstruction process of the high-frequency components, our method monitors errors caused in the known low-frequency components and realizes the selection of the optimal eigenspace. Then, since the missing high-frequency components can be adaptively estimated, the accurate HR image can be obtained.

Index Terms— Resolution enhancement, Image enlargement, Super-resolution, Kernel PCA.

1. INTRODUCTION

In the field of image processing, resolution enhancement of digital images is a very important issue, because it can be applied to fundamental applications. For example, many applications such as enlargement of consumer photographs and conversion of traditional standard-definition television video content to high-definition television could benefit from resolution enhancement techniques.

Many methods for achieving accurate resolution enhancement have been proposed in order to realize the above applications. Traditionally, nearest neighbor, bilinear, bicubic, and sinc interpolation methods [1, 2] have been utilized for image enlargement. However, since they cannot estimate missing high-frequency components of the original high-resolution (HR) image, their results suffer from some blurring. Thus, in order to estimate the missing high-frequency components, single-frame super-resolution methods have been proposed [3]. However, since these methods need to utilize other HR images as training data for reconstructing the high-frequency components, their performance depends on these training data.

In this paper, a novel resolution enhancement method based on a kernel PCA [4] is proposed. The proposed method introduces two novel approaches into the reconstruction of the missing high-frequency components. First, nonlinear eigenspaces calculated from local images in the target low-resolution (LR) image are utilized as those of the HR image. Specifically, our method classifies local images clipped from the target LR image into some clusters, and regards the nonlinear eigenspace of each cluster as that of the HR image. Since local images between two different resolution levels of a pyramid structure are similar to each other, the accurate estimation of the nonlinear eigenspaces of the HR image can be expected. Then,

by using each nonlinear eigenspace, the inverse mapping, which reconstructs the missing high-frequency components from the known low-frequency components, can be approximately calculated. Secondly, in the reconstruction process using the obtained inverse mapping, the proposed method adaptively selects a cluster minimizing errors of the known low-frequency components. This approach provides a solution for searching the optimal cluster even if the HR image is unknown. Consequently, utilizing the optimal cluster's inverse mapping, the proposed method can correctly reconstruct the high-frequency components. Therefore, in our method, the accurate estimation of the HR image can be expected.

This paper is organized as follows. The estimation of the nonlinear eigenspaces of the HR image is explained in Section 2. In Section 3, the new image resolution enhancement method using the obtained nonlinear eigenspaces is presented. Experimental results that verify the performance of the proposed method are shown in Section 4. Finally, conclusion remarks are shown in Section 5.

2. ESTIMATION OF NONLINEAR EIGENSPACES

In this section, we estimate eigenspaces of a HR image using only a target LR image. As shown in Fig. 1, the target LR image f , which we observe, is obtained by blurring and subsampling the HR image F . We can easily calculate the blurred HR image \hat{F} in Fig. 1 by upsampling the target LR image f . However, it is difficult to reconstruct F from \hat{F} since the high-frequency components of F are missed by the low-pass filter. Therefore, the proposed method tries to estimate the missing high-frequency components based on a nonlinear eigenspace method, which utilizes nonlinear eigenspaces of the HR image. Note that these eigenspaces cannot be directly calculated since the original HR image is unknown. Thus, we utilize eigenspaces calculated from local images in the target LR image for those of the HR image. It is well known that local images between two different resolution levels of a pyramid structure are similar to each other. Therefore, utilizing the eigenspaces calculated from the local images in the target LR image, the accurate estimation scheme of the eigenspaces of the HR image can be expected. The details of this estimation are described below.

First, we clip N local images g_i ($i = 1, 2, \dots, N$) whose size is $w \times h$ pixels from the target LR image f . Next, two images g_i^L and g_i^H , which respectively include low-frequency and high-frequency components of each clipped local image g_i , are calculated. Then, we obtain vectors \mathbf{l}_i and \mathbf{h}_i whose elements are respectively the raster scanned intensities of g_i^L and g_i^H . Furthermore, the proposed method maps \mathbf{l}_i into the feature space via the nonlinear map $\Phi: \mathbf{R}^{wh} \rightarrow \mathbf{F}$ [4], and defines a vector $\phi_i = [\Phi(\mathbf{l}_i)', \mathbf{h}_i']^T$. In this paper, we use the nonlinear map whose kernel function is a Gaussian kernel. Note that an

¹In this paper, vector/matrix transpose is denoted by the superscript '.

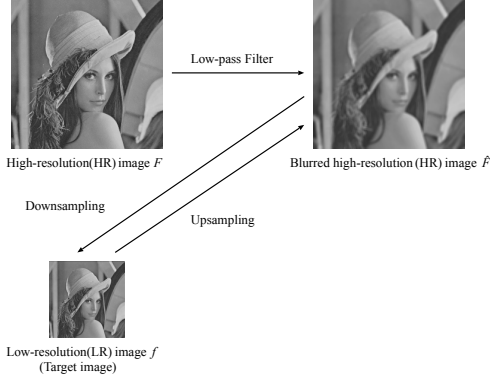


Fig. 1. Relationship between HR image F , blurred HR image \hat{F} , and LR image f .

exact pre-image, which is the inverse mapping from the feature space back to the input space, typically does not exist [5]. Therefore, the estimated pre-image includes some errors. Since the final results estimated in the proposed method are the missing high-frequency components, we do not utilize the nonlinear map for \mathbf{h}_i ($i = 1, 2, \dots, N$).

From the obtained results ϕ_i ($i = 1, 2, \dots, N$), the proposed method performs their classification that minimizes the following new criterion:

$$E_c = \sum_{k=1}^K \sum_{j=1}^{M^k} \|\mathbf{l}_j^k - \tilde{\mathbf{l}}_j^k\|^2 + \|\mathbf{h}_j^k - \tilde{\mathbf{h}}_j^k\|^2, \quad (1)$$

where K is the number of the clusters. The vectors \mathbf{l}_j^k and \mathbf{h}_j^k ($j = 1, 2, \dots, M^k$) respectively represent \mathbf{l}_i and \mathbf{h}_i of g_i ($i = 1, 2, \dots, N$) classified into cluster k . Further, the vectors $\tilde{\mathbf{l}}_j^k$ and $\tilde{\mathbf{h}}_j^k$ satisfy $\tilde{\phi}_j^k = [\Phi(\tilde{\mathbf{l}}_j^k)', \tilde{\mathbf{h}}_j^k']'$, and $\tilde{\phi}_j^k$ is obtained below.

$$\tilde{\phi}_j^k = \mathbf{U}^k \mathbf{U}^{k'} \left(\phi_j^k - \bar{\phi}^k \right) + \bar{\phi}^k, \quad (2)$$

where $\phi_j^k = [\Phi(\mathbf{l}_j^k)', \mathbf{h}_j^k']'$, and $\bar{\phi}^k$ is the mean vector, which is calculated from ϕ_j^k ($j = 1, 2, \dots, M^k$) as follows:

$$\bar{\phi}^k = \frac{1}{M^k} \Xi^k \mathbf{1}^k. \quad (3)$$

In the above equation, $\Xi^k = [\phi_1^k, \phi_2^k, \dots, \phi_{M^k}^k]$ and $\mathbf{1}^k = [1, 1, \dots, 1]'$ is an $M^k \times 1$ vector. Further,

$$\mathbf{U}^k = [\mathbf{u}_1^k, \mathbf{u}_2^k, \dots, \mathbf{u}_{D^k}^k] \quad (D^k < M^k) \quad (4)$$

is an eigenvector matrix of $\Xi^k \mathbf{H}^k \mathbf{H}^k \Xi^{k'}$, where \mathbf{H}^k is a centering matrix defined as follows:

$$\mathbf{H}^k = \mathbf{I}^k - \frac{1}{M^k} \mathbf{1}^k \mathbf{1}^{k'}, \quad (5)$$

where \mathbf{I}^k is the $M^k \times M^k$ identity matrix.

In Eq. (4), the eigenvectors \mathbf{u}_d^k ($d = 1, 2, \dots, D^k$) are high-dimensional, and Eq. (2) therefore cannot be calculated directly. Thus, we introduce the computational scheme ‘‘kernel trick’’ [4] into the calculation of Eq. (2). The eigenvector matrix \mathbf{U}^k satisfies the following singular value decomposition:

$$\Xi^k \mathbf{H}^k \Xi^{k'} \cong \mathbf{U}^k \Lambda^k \mathbf{V}^{k'}, \quad (6)$$

where Λ^k is the eigenvalue matrix and \mathbf{V}^k is the eigenvector matrix of $\mathbf{H}^k \Xi^{k'} \Xi^k \mathbf{H}^k$. Therefore, \mathbf{U}^k can be obtained as follows:

$$\mathbf{U}^k \cong \Xi^k \mathbf{H}^k \mathbf{V}^k \Lambda^{k-1}. \quad (7)$$

Then, from Eqs. (3) and (7), Eq. (2) can be written as

$$\begin{aligned} \tilde{\phi}_j^k &\cong \Xi^k \mathbf{H}^k \mathbf{V}^k \Lambda^{k-2} \mathbf{V}^{k'} \mathbf{H}^k \Xi^{k'} \left(\phi_j^k - \frac{1}{M^k} \Xi^k \mathbf{1}^k \right) + \frac{1}{M^k} \Xi^k \mathbf{1}^k \\ &= \Xi^k \mathbf{W}^k \Xi^{k'} \left(\phi_j^k - \frac{1}{M^k} \Xi^k \mathbf{1}^k \right) + \frac{1}{M^k} \Xi^k \mathbf{1}^k, \end{aligned} \quad (8)$$

where

$$\mathbf{W}^k = \mathbf{H}^k \mathbf{V}^k \Lambda^{k-2} \mathbf{V}^{k'} \mathbf{H}^k. \quad (9)$$

In this way, we can calculate Eq. (2). Next, in Eq. (1), $\|\mathbf{l}_j^k - \tilde{\mathbf{l}}_j^k\|^2$ satisfies the following equation of the Gaussian kernel [4]:

$$\Phi(\mathbf{l}_j^k)' \Phi(\tilde{\mathbf{l}}_j^k) = \exp \left\{ -\frac{\|\mathbf{l}_j^k - \tilde{\mathbf{l}}_j^k\|^2}{\sigma_1^2} \right\}. \quad (10)$$

Given $\Xi_1^k = [\Phi(\mathbf{l}_1^k), \Phi(\mathbf{l}_2^k), \dots, \Phi(\mathbf{l}_{M^k}^k)]$ and $\Xi_{\mathbf{h}}^k = [\mathbf{h}_1^k, \mathbf{h}_2^k, \dots, \mathbf{h}_{M^k}^k]$, they satisfy $\Xi^k = [\Xi_1^k, \Xi_{\mathbf{h}}^k]'$. Thus, from Eq. (8), $\Phi(\tilde{\mathbf{l}}_j^k)$ in Eq. (10) is obtained as follows:

$$\Phi(\tilde{\mathbf{l}}_j^k) \cong \Xi_1^k \mathbf{W}^k \Xi^{k'} \left(\phi_j^k - \frac{1}{M^k} \Xi^k \mathbf{1}^k \right) + \frac{1}{M^k} \Xi_1^k \mathbf{1}^k. \quad (11)$$

Then, by using Eqs. (10) and (11), $\|\mathbf{l}_j^k - \tilde{\mathbf{l}}_j^k\|^2$ in Eq. (1) can be obtained as follows:

$$\begin{aligned} \|\mathbf{l}_j^k - \tilde{\mathbf{l}}_j^k\|^2 &\cong -\sigma_1^2 \log \left\{ \Phi(\mathbf{l}_j^k)' \Xi_1^k \mathbf{W}^k \Xi^{k'} \left(\phi_j^k - \frac{1}{M^k} \Xi^k \mathbf{1}^k \right) \right. \\ &\quad \left. + \frac{1}{M^k} \Phi(\mathbf{l}_j^k)' \Xi_1^k \mathbf{1}^k \right\}. \end{aligned} \quad (12)$$

Furthermore, since $\tilde{\mathbf{h}}_j^k$ is calculated from Eq. (8) as

$$\tilde{\mathbf{h}}_j^k \cong \Xi_{\mathbf{h}}^k \mathbf{W}^k \Xi^{k'} \left(\phi_j^k - \frac{1}{M^k} \Xi^k \mathbf{1}^k \right) + \frac{1}{M^k} \Xi_{\mathbf{h}}^k \mathbf{1}^k, \quad (13)$$

$\|\mathbf{h}_j^k - \tilde{\mathbf{h}}_j^k\|^2$ in Eq. (1) is also obtained as follows:

$$\|\mathbf{h}_j^k - \tilde{\mathbf{h}}_j^k\|^2 \cong \left\| \mathbf{h}_j^k - \Xi_{\mathbf{h}}^k \mathbf{W}^k \Xi^{k'} \left(\phi_j^k - \frac{1}{M^k} \Xi^k \mathbf{1}^k \right) - \frac{1}{M^k} \Xi_{\mathbf{h}}^k \mathbf{1}^k \right\|^2 \quad (14)$$

Then, from Eqs. (12) and (14), the criterion E_c in Eq. (1) can be calculated.

In Eq. (2), $\mathbf{U}^k \mathbf{U}^{k'}$ is the projection matrix onto the eigenspace spanned by their eigenvectors \mathbf{u}_d^k ($d = 1, 2, \dots, D^k$). Therefore, the criterion E_c represents the sum of the approximation errors of ϕ_j^k ($j = 1, 2, \dots, M^k$) in their eigenspaces. This means that the squared error in Eq. (1) corresponds to the distance from the nonlinear eigenspace of each cluster in the input space. Then, the new criterion E_c is useful for classification of the local images. From the classification results, we can estimate the nonlinear eigenspaces of the HR image by calculating the eigenvector matrices \mathbf{U}^k ($k = 1, 2, \dots, K$).

3. KERNEL PCA-BASED HR IMAGE ESTIMATION

In this section, we show a new estimation method of the HR image by utilizing the nonlinear eigenspaces calculated in the previous section. Given two local images G and \hat{G} ($w \times h$ pixels) respectively clipped from the same position of the HR image and the blurred HR image shown in Fig. 1, they satisfy the following equation:

$$\begin{aligned}\hat{\phi} &= \begin{bmatrix} \mathbf{I} & \mathbf{0} \\ \mathbf{0} & \mathbf{0} \end{bmatrix} \phi \\ &= \Sigma \phi,\end{aligned}\quad (15)$$

where the vector $\phi (= [\Phi(\mathbf{I})', \mathbf{h}']')$ and $\hat{\phi} (= [\Phi(\mathbf{I})', \mathbf{0}']')$ are respectively calculated from G and \hat{G} by the same way as ϕ_i ($i = 1, 2, \dots, N$) in the previous section. In Eq. (15), since the matrix Σ is not regular, we cannot directly calculate its inverse matrix to estimate the missing high-frequency components \mathbf{h} and obtain the original HR image. Thus, the proposed method projects ϕ and $\hat{\phi}$ onto the nonlinear eigenspace of cluster k , and newly defines the matrix, which corresponds to Σ , in the nonlinear eigenspace. Then, if the defined matrix becomes regular, its inverse matrix can be calculated. Therefore, since the missing high-frequency components are also calculated approximately, the accurate reconstruction of the HR image can be expected. We show the specific algorithm of the proposed method in the rest of this section.

The vectors ϕ and $\hat{\phi}$ can be projected onto the D^k -dimensional nonlinear eigenspace of cluster k by using the nonlinear eigenvector matrix \mathbf{U}^k as follows:

$$\mathbf{p} = \mathbf{U}^{k'} (\phi - \bar{\phi}^k), \quad (16)$$

$$\hat{\mathbf{p}} = \mathbf{U}^{k'} (\hat{\phi} - \bar{\phi}^k). \quad (17)$$

Further, ϕ is approximately calculated as follows:

$$\phi \cong \mathbf{U}^k \mathbf{p} + \bar{\phi}^k. \quad (18)$$

Next, by substituting Eqs. (15) and (18) into Eq. (17), the following equation is obtained:

$$\hat{\mathbf{p}} \cong \mathbf{U}^{k'} \Sigma (\mathbf{U}^k \mathbf{p} + \bar{\phi}^k) - \mathbf{U}^{k'} \bar{\phi}^k. \quad (19)$$

Thus,

$$\mathbf{U}^{k'} \Sigma \mathbf{U}^k \mathbf{p} \cong \hat{\mathbf{p}} - \mathbf{U}^{k'} \Sigma \bar{\phi}^k + \mathbf{U}^{k'} \bar{\phi}^k. \quad (20)$$

In the above equation, if the matrix $\mathbf{U}^{k'} \Sigma \mathbf{U}^k$ is regular, its inverse matrix $(\mathbf{U}^{k'} \Sigma \mathbf{U}^k)^{-1}$ can be calculated, and the following equation is obtained.

$$\mathbf{p} \cong (\mathbf{U}^{k'} \Sigma \mathbf{U}^k)^{-1} \hat{\mathbf{p}} + (\mathbf{U}^{k'} \Sigma \mathbf{U}^k)^{-1} \mathbf{U}^{k'} (\bar{\phi}^k - \Sigma \bar{\phi}^k). \quad (21)$$

Finally, by substituting Eqs. (16) and (17) into the above equation, the following equation can be obtained:

$$\mathbf{U}^{k'} (\phi - \bar{\phi}^k) \cong (\mathbf{U}^{k'} \Sigma \mathbf{U}^k)^{-1} \mathbf{U}^{k'} (\hat{\phi} - \Sigma \bar{\phi}^k). \quad (22)$$

Then, we can calculate an approximation result $\phi^k (= [\phi_1^{k'}, \mathbf{h}^{k'}]')$ of ϕ from cluster k 's eigenspace as follows:

$$\phi^k \cong \mathbf{U}^k (\mathbf{U}^{k'} \Sigma \mathbf{U}^k)^{-1} \mathbf{U}^{k'} (\hat{\phi} - \Sigma \bar{\phi}^k) + \bar{\phi}^k. \quad (23)$$

Further, by utilizing Eq. (7), we can obtain the following equation:

$$\phi^k \cong \Xi^k \mathbf{T}^k \Xi^{k'} (\hat{\phi} - \Sigma \bar{\phi}^k) + \bar{\phi}^k, \quad (24)$$

where \mathbf{T}^k is calculated as follows:

$$\mathbf{T}^k = \mathbf{H}^k \mathbf{V}^k (\mathbf{V}^{k'} \mathbf{H}^{k'} \Xi^{k'} \Sigma \Xi^k \mathbf{H}^k \mathbf{V}^k)^{-1} \mathbf{V}^{k'} \mathbf{H}^k. \quad (25)$$

Note that the estimation result, which we have to estimate, is the vector \mathbf{h} of the unknown high-frequency components. Since Eq. (24) is rewritten as

$$\begin{bmatrix} \phi_1^k \\ \mathbf{h}^k \end{bmatrix} \cong \begin{bmatrix} \Xi_1^k \\ \Xi_{\mathbf{h}}^k \end{bmatrix} \mathbf{T}^k \Xi^{k'} (\hat{\phi} - \Sigma \bar{\phi}^k) + \begin{bmatrix} \bar{\phi}_1^k \\ \bar{\mathbf{h}}^k \end{bmatrix}, \quad (26)$$

where $\bar{\phi}^k = [\bar{\phi}_1^{k'}, \bar{\mathbf{h}}^{k'}]'$. Thus, from Eqs. (3) and (26), the vector \mathbf{h}^k , which is the estimation result of \mathbf{h} by cluster k , is calculated as follows:

$$\mathbf{h}^k \cong \Xi_{\mathbf{h}}^k \mathbf{T}^k \Xi^{k'} \left(\hat{\phi} - \frac{1}{M^k} \Xi_1^k \mathbf{1}^k \right) + \frac{1}{M^k} \Xi_{\mathbf{h}}^k \mathbf{1}^k. \quad (27)$$

Then, utilizing the nonlinear eigenspace of cluster k , the proposed method can estimate the missing high-frequency components.

In the least-squares sense, the nonlinear eigenspace of cluster k correctly approximates ϕ_j^k ($j = 1, 2, \dots, M^k$) belonging to the same cluster k . Therefore, if we can classify ϕ of the target local image G , the proposed method accurately reconstructs the missing high-frequency components \mathbf{h} by using the nonlinear eigenspace of the cluster including ϕ . Unfortunately, since the vector, which can be utilized for the classification, is only $\hat{\phi}$, ϕ cannot be classified by the algorithm shown in the previous section. Thus, in order to achieve the classification of ϕ , the proposed method utilizes the following novel criterion as a substitute for Eq. (1).

$$\tilde{E}^k = \|\mathbf{l} - \mathbf{l}^k\|^2. \quad (28)$$

In the above equation, $\|\mathbf{l} - \mathbf{l}^k\|^2$ is satisfied as follows:

$$\Phi(\mathbf{I})' \phi_1^k = \exp \left\{ -\frac{\|\mathbf{l} - \mathbf{l}^k\|^2}{\sigma_1^2} \right\}, \quad (29)$$

and ϕ_1^k is calculated from Eqs. (3) and (26) below.

$$\phi_1^k \cong \Xi_1^k \mathbf{T}^k \Xi^{k'} \left(\hat{\phi} - \frac{1}{M^k} \Sigma \Xi^k \mathbf{1}^k \right) + \frac{1}{M^k} \Xi_1^k \mathbf{1}^k. \quad (30)$$

Then, from Eqs. (29) and (30), the criterion \tilde{E}^k in Eq. (28) can be rewritten as follows:

$$\tilde{E}^k \cong -\sigma_1^2 \log \left\{ \Phi(\mathbf{I})' \Xi_1^k \mathbf{T}^k \Xi^{k'} (\hat{\phi} - \Sigma \bar{\phi}^k) + \frac{1}{M^k} \Phi(\mathbf{I})' \Xi_1^k \mathbf{1}^k \right\}. \quad (31)$$

This criterion \tilde{E}^k is the squared error calculated between the low-frequency components \mathbf{l}^k reconstructed with the high-frequency components \mathbf{h}^k by cluster k 's nonlinear eigenspace and the known original low-frequency components \mathbf{l} . Therefore, \tilde{E}^k is suitable for evaluating the cluster k and applicable for the classification of the target local image. Then, the selection of the optimal cluster for the target local image whose high-frequency components are unknown becomes possible. Furthermore, the proposed method regards the result ϕ^k minimizing \tilde{E}^k as the output $\phi^* (= [\phi_1^{*'}, \mathbf{h}^{*'}]')$. Then, $\mathbf{l} + \mathbf{h}^*$ is the estimated vector whose elements are the raster scanned intensities of the target local image in the HR image.

As described above, we can reconstruct the target local image of the HR image. The proposed method clips local images ($w \times h$ pixels) at the same interval in a raster scanning order from the blurred HR image. Further, each local image is reconstructed by the above schemes. Note that each pixel has multiple estimation results if the clipping interval is smaller than the size of the local images. In this case, the proposed method regards the result minimizing Eq. (31) as the final result. Then, we can realize the resolution enhancement of the target LR image.

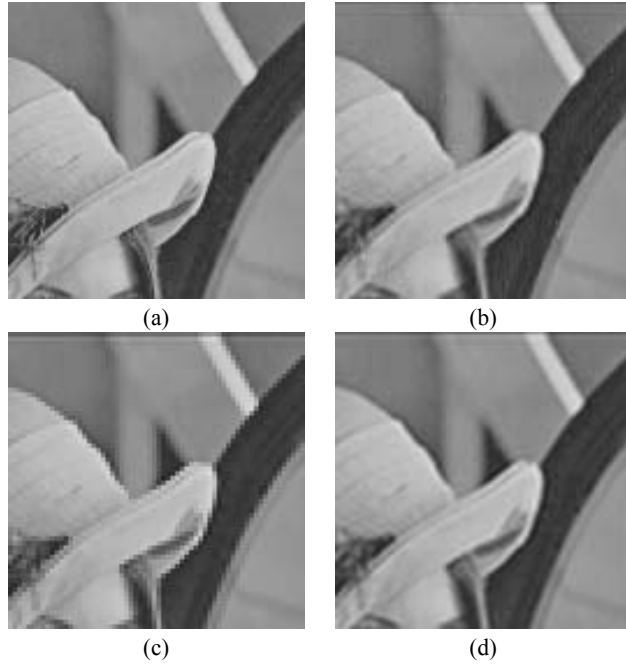


Fig. 2. (a) Original Lena image, (b) Estimated HR image by the proposed method (31.53 dB), (c) Estimated HR image by the nearest neighbor interpolation method (26.23 dB), (d) Estimated HR image by the sinc interpolation method (31.43 dB).

4. EXPERIMENTAL RESULTS

The performance of the proposed method is verified in this section. We use test images “Lena” and “Baboon” of size 256×256 pixels and 8bits/pixel as HR images. In order to obtain LR images, we subsample the test images to the size of 128×128 pixels by using the sinc filter with the hamming window. Next, we apply the proposed method² to the target images of size 128×128 pixels and obtain the enlarged results of size 256×256 pixels. We show the estimated HR image of “Lena” in Fig. 2(b). Note that the enlarged portions around the hat of “Lena” are shown in Fig. 2 for better subjective evaluation. For comparison, we show Figs. 2(c) and (d), which are respectively obtained by the traditional nearest neighbor and sinc interpolation [2] methods. Further, another experimental result performed for “Baboon” is shown in Fig. 3. From these figures, we can see that the proposed method preserves the sharpness more successfully than the traditional methods.

Since the traditional methods cannot estimate the missing high-frequency components of the original HR images from the LR images, their reconstructed HR images suffer from some blurring. On the other hand, the proposed method estimates the missing high-frequency components by utilizing the correlation between two different resolution levels of a pyramid structure, effectively.

Finally, as shown in the captions of Figs. 2 and 3, the proposed method achieves 0.08 and 1.57 dB improvement over the best published method, respectively. Therefore, our method realizes the accurate resolution enhancement subjectively and objectively.

²We set the parameters of the proposed method as follows: σ_1^2 is set to the variance $\|I_i - I_j\|^2$ ($i, j = 1, 2, \dots, N$), and $K = 6$.

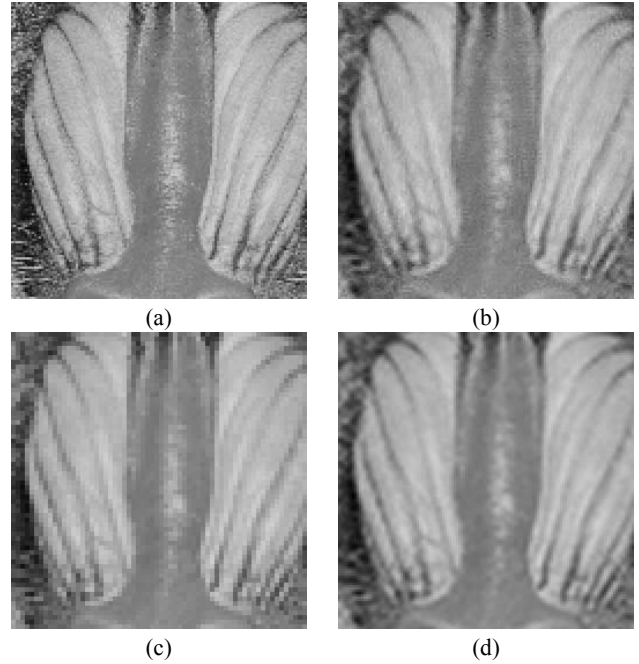


Fig. 3. (a) Original Baboon image, (b) Estimated HR image by the proposed method (25.78 dB), (c) Estimated HR image by the nearest neighbor interpolation method (24.21 dB), (d) Estimated HR image by the sinc interpolation method (23.42 dB).

5. CONCLUSIONS

In this paper, we have proposed a new kernel PCA-based framework for image resolution enhancement in still images. We note the correlation between two different resolution levels of a pyramid structure, and realize the estimation of nonlinear eigenspaces of the HR image from only the observed target LR image. Further, using the optimal nonlinear eigenspace adaptively selected by the novel criterion, the proposed method can accurately calculate the inverse mapping, which reconstructs the missing high-frequency components from the known low-frequency components. Therefore, the accurate HR image can be obtained. Consequently, we can confirm the improvement of the proposed technique over previously reported technique. In future work, reduction of computational cost is needed for practical use of the proposed method.

6. REFERENCES

- [1] R. G. Keys, “Cubic convolution interpolation for digital image processing,” *IEEE Trans. Acoust., Speech, Signal Processing*, vol. ASSP-29, pp. 1153-1160, Dec. 1981.
- [2] Oppenheim, A. V. and Schaffer, R. W., “Discrete-Time Signal Processing, 2nd Edition,” *Prentice Hall, New Jersey*, 1999.
- [3] W. T. Freeman, T. R. Jones and E. C. Pasztor, “Example-based super-resolution,” *IEEE Computer Graphics and Applications*, vol.22, no.2, pp.56-65, 2002.
- [4] B. Schölkopf, S. Mika, C.J.C Burges, P. Knirsch, K.-R. Müller, G. Rätsch, and A.J. Smola, “Input space versus feature space in kernel-based methods,” *IEEE Trans. on Neural Networks*, vol.10, no.5, pp.1000-1017, 1999.
- [5] J.T.-Y. Kwok, I.W.-H. Tsang, “The pre-image problem in kernel methods,” *IEEE Trans. on Neural Networks*, vol.15, no.6, pp.1517-1525, 2004.